Pergamon

Int. J. Solids Structures Vol. 31, No. 18, pp. 2565–2587, 1994

0020–7683/94 $7.00 + .00

0020–7683(94)E0042–T

EFFECTS OF ADHEREND DEFLECTIONS IN SINGLE LAP JOINTS

D. W. OPLINGER
Federal Aviation Administration Technical Center, Atlantic City International Airport, NJ 08405, U.S.A.

(*Received* 10 *May* 1993; *in revised form* 18 *March* 1994)

Abstract—The well-known analysis of the single lap joint by Goland and Reissner provided important contributions to the literature on stress analysis of adhesive joints by clarifying not only the importance of adhesive peel stresses in joint failure, but also the role of bending deflections of the joint in controlling the level of the stresses in the adhesive layer. Subsequent efforts have suggested the need for corrections to the Goland and Reissner analysis because of what have been conceived as deficiencies in the model used to describe bending deflections of the central part of the joint where a classical homogeneous beam model without shear or thickness normal deflections was used. The present paper addresses the issue through the use of a more realistic model in which adhesive layer deflections are allowed to decouple the two halves of the joint in the bending deflection analysis, as well as in the analysis of adhesive layer stresses where such a decoupling was allowed by Goland and Reissner. It is found that many of the predictions of the Goland–Reissner analysis are recovered in the limit of large adherend-to-adhesive layer thickness ratios, although substantial differences from the Goland–Reissner analysis can occur for relatively thin adherends.

NOMENCLATURE

B_U, B_L	stretching stiffness, upper, lower adherend ($\equiv E't$)
D_U, D_L	bending stiffness, upper, lower adherend ($\equiv E't^3/12$)
E	adherend Young's modulus
E' [$\equiv E/(1-\nu^2)$]	adherend plane strain Young's modulus
E_b	bond layer Young's modulus
G_b	bond layer shear modulus
L ($\equiv l_0+l/2$)	half length of joint (see Fig. 2)
M_U, M_L	moments in individual adherends
M_0	moments in loaded adherend at ends of overlap
R	ratio, U/β
R_j (j = 1, 2)	ratios of roots μ_j to $U/(8)^{1/2}$ (j = 1) or $(8)^{1/2}\beta$
T_U, T_L	adherend resultants, $t\sigma_x$
$\bar{T}$ (x = 0, 2L)	resultants applied at ends of joint
T_Δ [(eqn (3)]	$T_U - T_L$
U [eqn (23)]	$t(T/D_U)^{1/2} \equiv (12\bar{\varepsilon}_x)^{1/2}$
$\bar{V}$	lateral loads at ends of joint (see Fig. 2)
V_0	lateral loads at ends of overlap
c	$l/2$ in GR notation
h	height (combined thickness) of overlap region in thickness direction
k [eqn (25.1)]	ratio of M_0 to $\bar{T}t/2$ or of displacement at ends of overlap to $t/2$
k_1, k_2 [eqn (25.2)]	ratios of displacement solution coefficients to $t/2$
l (Fig. 2)	axial length of overlap region
l_0 (Fig. 2)	axial length of outer section of adherends
t	adherend thickness
t_b	bond layer thickness
u	axial displacement
w [eqns (3)]	$(w_U + w_L)/2$
w_U, w_L	adherend lateral displacements
x	axial coordinate
z	thickness-wise coordinate
Δ_{hj} [eqns (22)]	coefficients of solution for T_Δ
β [eqn(23)]	$(\rho_G/\rho_t)^{1/2}$
$\bar{\varepsilon}_x$ [eqn (1.2)]	nominal applied strain, $\bar{\sigma}_x/E'$
γ_b	bond layer shear strain
λ	dimensionless overlap length l/t
λ_0	dimensionless length of outer adherend segment l_0/t
μ_1, μ_2 [eqns (27)]	exponential coefficients of differential equations for w and T_Δ
μ_{G1}, μ_{G2} [eqns (28)]	$U/8^{1/2}$, $8^{1/2}\beta$, respectively
ρ_G	modulus ratio E'/G_b

ρ_t	thickness ratio t_b/t
σ_x [eqn (1.1)]	nominal applied stress in adherend

INTRODUCTION

One of the most widely quoted papers in the literature on stresses in adhesive joints is that of Goland and Reissner (1944) (subsequently referred to as "GR") on single lap joints. This paper was particularly significant in drawing attention to the effects of adherend bending deflections on the peel and shear stresses in the adhesive layer of a single lap joint. The segment of the GR analysis of interest here is a combination of parts 1 and 3 of GR, which provided a beam model for predicting deflections in the joint and, subsequently, shear and peel stresses in the bond layer. (Part 2 was an approximate elasticity analysis based on a Green's function approach which dealt with ideally rigid adhesives, with the adherends essentially welded together.)

Part 1 of the GR analysis relating to bending deflections treated the actual joint, Fig. 1(A), as a stepped homogeneous beam, Fig. 1(B), in which the height of the center section was assumed to be twice the thickness of the adherends (thus ignoring the thickness of the bond layer). The forces due to tensile end loading, assumed to lie along the line a–a′ in Fig. 1(A), were found to produce varying moment about the neutral axis at any point along the representative beam, which resulted in the bending deflections of interest. The deflection analysis for this system was treated essentially by "beam column" analysis, i.e. as the analysis of deflections in a column with offset loading, in tension rather than compression, the latter being the usual case of interest in beam column analysis.

A question arises with the GR analysis regarding the manner in which the moment is represented in the center section, namely, by a classical Euler beam moment–curvature relationship which represents the overlapping region as a homogeneous beam having no influence of transverse shear or thickness-wise deflections. Hart-Smith (1973) suggested that such an approach was inconsistent with the force and moment conditions of the individual adherends at either end of the overlap. To deal with this situation, Hart-Smith provided a modified analysis that led to predictions for the lateral deflections of the system which departed radically from those of the GR analysis. Hart-Smith has used this approach in numerous discussions of the single lap joint since it was first presented.

In his modified analysis, Hart-Smith treated the individual adherends as decoupled beams in order to apply end conditions to the adherends independently as a means of correcting what were perceived to be the deficiencies of the GR analysis. In the course of this analysis, the effect of bending deflections on the moment distribution in the overlap region was omitted. The departure of the Hart-Smith predictions from those of GR was

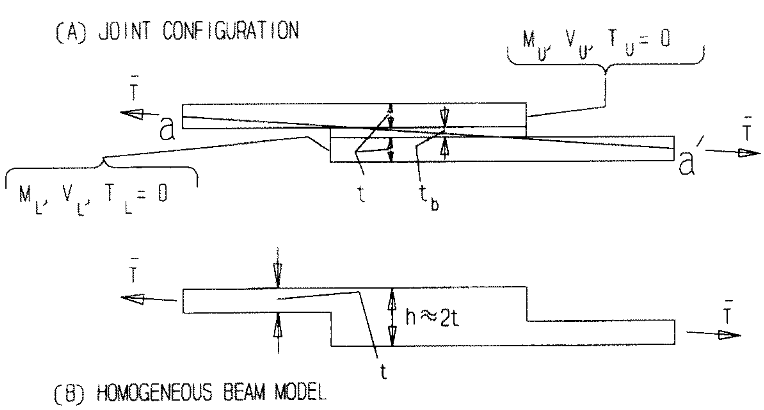

Fig. 1. Assumed model.

strongly influenced by this aspect of the analysis and needs to be reconsidered. In the present paper, the issue of the influence of bending deflections in the single lap joint is re-examined, using an approach which departs from the Euler beam model of the overlap region used by GR, by introducing the effect of shear deflections of the bond layer as a means of decoupling the bending response of the individual adherends, while retaining the influence of lateral deflections on the moment distribution in the overlap region as well as in the remainder of the joint. The resulting formulation provides an alternative method of correcting for the deficiencies which Hart-Smith perceived in the GR bending analysis, while maintaining a realistic treatment of the moment distribution in the center parts of the joint. A comparison of the two approaches will be given subsequently. It is found that the present approach leads to predictions which differ considerably from the Hart-Smith approach while retaining much of the character of the original GR analysis. In addition to the discussion of Hart-Smith, problems with the GR treatment of the bending analysis have been noted by others (Benson, 1969; Adams and Wake, 1984). Benson (1969), as discussed by Adams and Wake (1984), described a modification of the analysis which dealt with the situation but did not provide for the effect of shear strains on deflections.

Along with Benson (1969) and Adams and Wake (1984), a number of analytical efforts (Kuenzi and Stevens, 1963; Kutscha and Hofer, 1968; Sneddon, 1962) on adhesive joints have suggested additional shortcomings of the GR analysis, in this case with regard to the GR predictions of peel stresses, which do not appear to be valid to the writer. As suggested by Carpenter (1989) and by Tsai and Morton (1994), these apparently arose because of misprints in the GR paper which implied incorrect expressions for peel stresses. In fact, the correct peel stress equations appear to have been stated in the final results given by GR as a result of the compensating effects of successive misprints.

This paper is a slightly condensed version of the Government report presented in Oplinger (1991). In addition, it is noted that Tsai and Morton (1994) have generated large-deflection finite element predictions which gave good comparisons with the analytical expressions of the present paper.

The present effort is admittedly limited in scope, in restricting its objective to providing an alternative to the Hart-Smith modification of the original GR analysis. Here, various effects which might be of interest are not dealt with; for example, transverse shear deformations in the adherends are not taken into account, with the result that the analysis applies primarily to metal adherends. Carpenter (1991) reported that adherend transverse shear deformations had a sizeable effect on peel stresses in some joint configurations. However, the writer has evaluated a simple correction for adherend transverse shear deformations which suggests that they can be accounted for by an effective reduction of the bond shear modulus equivalent to dividing the actual shear modulus by a factor of $1/(1+G_b t/3G_{xz}t_b)$, where t_b and G_b are bond thickness and shear modulus, and t and G_{xz} are adherend thickness and shear modulus. This correction gives results in good agreement with finite element results for various joints, indicating that transverse shear effects are controlled by the adherend-to-bond thickness ratio as well as the bond-to-adherend shear modulus ratio, and will be important primarily for organic matrix composites; for metals which have a much smaller ratio of G_b to G_{xy}, the correction will be fairly minor.

In addition to transverse shear deformations in the adherends, Hart-Smith [see Hart-Smith (1981), for example] has generated an extensive body of information which shows that ductile behavior of the bond layer has a significant effect on the strength of adhesive joints and needs to be considered; the writer has developed a modification of the present analysis to allow for the effects of ductile adhesive response, which will be the subject of a future publication. Furthermore, in Adams and Wake (1984) as well as Tsai and Morton (1993), it was shown that the fillet at the end of the overlap has a major effect on the adhesive layer stresses near the ends of the overlap, and allowance for those effects is in order. The use of a finite element approach is called for in this instance, however. Furthermore, single lap joint test specimens for adhesive characterization are usually fabricated with the fillet eliminated, so that results applying to the single lap joint with no fillet are relevant for interpreting the behavior of such test specimens. Since the main interest here was to carry the classical one-dimensional continuum analysis as far as possible in the spirit of the original GR analysis, the use of the finite element approach to take the fillet into account has been avoided.

ANALYTIC FORMULATION

General remarks

Figure 2 gives the basic parameters of interest. Here "U" and "L" denote the "upper" and "lower" adherends. The length of the adherends beyond the overlap is l_0 while the overlap has a length l ($\equiv 2c$, in the GR notation). It is assumed that tension loads (i.e. resultants) $\bar{T}$ are present at the outer ends. In terms of $\bar{T}$, it is convenient to define nominal axial stress, $\bar{\sigma}_x$, and strain, $\bar{\varepsilon}_x$:

$$\bar{\sigma}_x = \frac{\bar{T}}{t} \quad (1.1); \quad \bar{\varepsilon}_x = \frac{\bar{\sigma}_x}{E'} \quad (1.2); \quad E' = E/(1-\nu^2) \quad (1.3)$$

(E, ν = Young's modulus, Poisson ratio for axial straining.)

Along with $\bar{T}$, there are assumed to be transverse shear forces $\bar{V}$ which produce moment free conditions at the end points, provided

$$\bar{V} = \alpha\bar{T}; \quad \alpha = (t+t_b)/2L; \quad L = l_0 + l/2 \equiv l_0 + c. \tag{2}$$

As in Fig. 2, the directions of the transverse forces are downward at the right end and upward at the left end for moment free conditions.

Figure 3(A) indicates the required symmetry of the transverse shear force, $V(x)$ [i.e. $V_R \equiv V(l-x) = V(x)$], about the centerline of the joint in the horizontal direction, while Fig. 3(B) recalls the antisymmetric nature of lateral displacement [$W_R \equiv w(l-x) = -W_L \equiv w(x)$]. These relationships lead to the end conditions on the adherends in the overlap region stated in Table 1. Note that the last four rows of Table 1 are used in forming the boundary conditions for the peel stress equations presented below.

Special notation

In the following discussion, it will be convenient to represent the individual adherend displacements and stress resultants in terms of differences and sums, since the bond layer stresses are more easily represented by differences in the adherend displacements and resultants than in terms of their individual values. Accordingly, the following notation is introduced:

$$T_\Delta(x) = T_U - T_L; \quad w(x) = \tfrac{1}{2}(w_U + w_L). \tag{3}$$

Note that the individual adherend resultants can be expressed in terms of $\bar{T}$ and $T_\Delta(x)$, as follows:

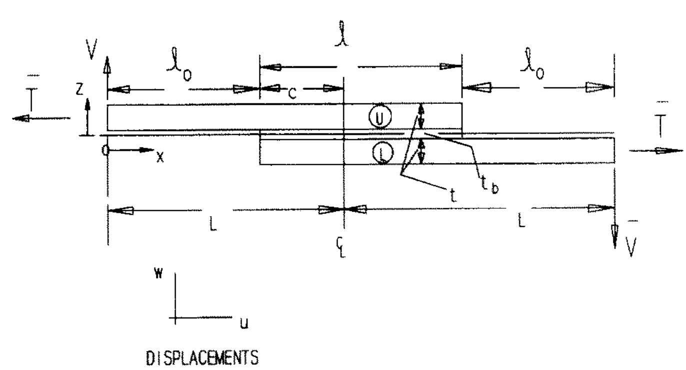

Fig. 2. Joint geometry.

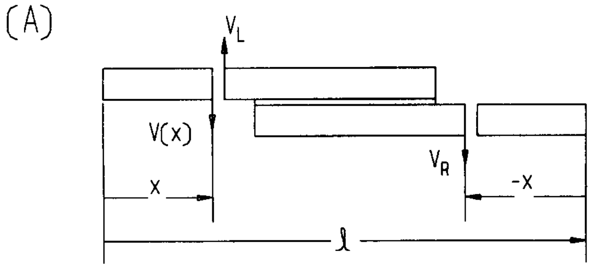

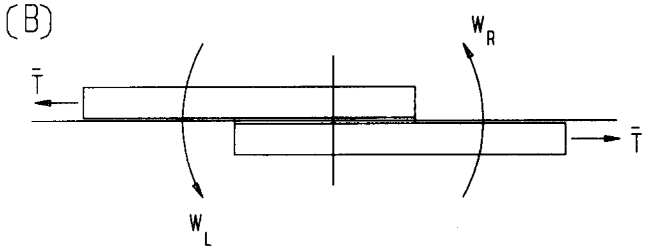

Fig. 3. Antisymmetry conditions.

$$T_U = \tfrac{1}{2}[\bar{T}+T_\Delta(x)]\,; \quad T_L = \tfrac{1}{2}[\bar{T}-T_\Delta(x)]. \tag{4}$$

Moment distribution

As in GR, the moment distribution along the joint is related to loads and displacements by (see Fig. 4):

outer end of upper adherend ($0 < x < l_0$)

$$M_U = \bar{T}(\alpha x+w)\,; \tag{5.1}$$

moment about neutral axis in overlap region ($l_0 < x < l_0+l$)

$$M_N = \bar{T}\alpha x+\left(w-\frac{t+t_b}{2}\right)\bar{T}\,; \tag{5.2}$$

outer end of lower adherend ($l_0+l < x < 2l_0+l$)

$$M_L = \bar{T}(\alpha x+w). \tag{5.3}$$

Strictly speaking, the thickness deformations of the bond layer, amounting to $t_b\sigma_b/E_b$

Table 1. Conditions on adherends at ends of overlap

	$x = l_0$	$x = l_0+l$
V_U	$-V_0 \equiv -UM_0/t$	0
M_U	$M_0 \equiv kt\bar{T}/2$	0
T_U	$\bar{T}$	0
V_L	0	$-V_0 \equiv -UM_0/t$
M_L	0	$-M_0 \equiv kt\bar{T}/2$
T_L	0	$\bar{T}$
M_U+M_L	M_0	$-M_0$
T_L-T_U	$-\bar{T}$	$\bar{T}$
M_U-M_L	M_0	M_0
V_U-V_L	$-V_0$	V_0

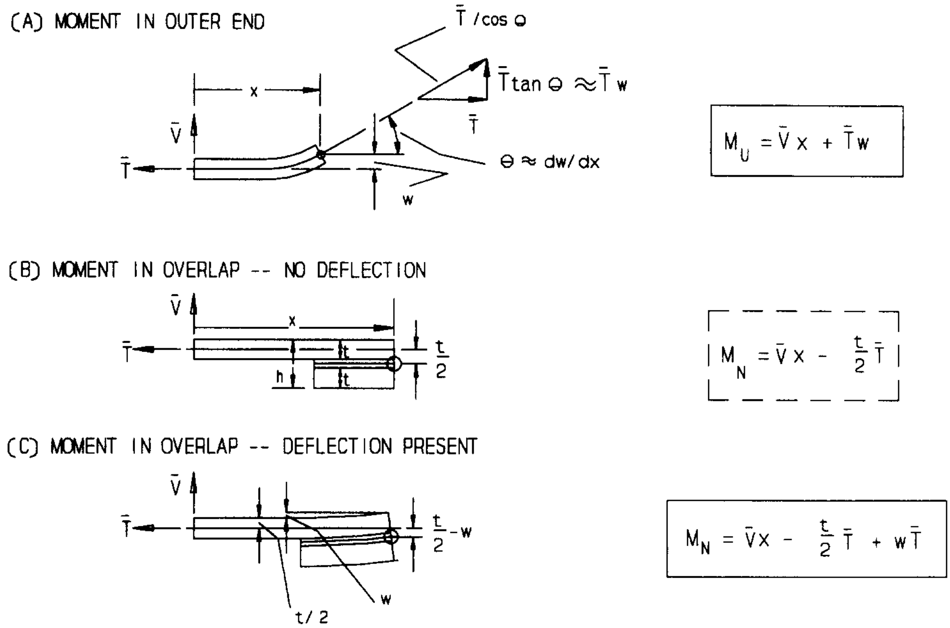

Fig. 4. Effect of deflection on moment distribution.

[see eqns (17) below] should be added to the term t_b in eqn (5.2), but are ignored as inconsequential.

Moment–curvature relation in the overlap region

The crux of the present approach involves representing the moment in the overlap region in terms of the moments and resultants in the individual adherends shown in Fig. 5. From equilibrium, M_N, the moment about the neutral axis in the overlap region, is given in terms of these parameters by

$$M_N = M_U + M_L + \frac{t+t_b}{2}(T_L - T_U). \tag{6}$$

Note that for $x = l_0$ where $M_L = 0 = T_L$, the expression for M_N here reduces to $M_N = M_U - (t+t_b)T_U/2$ which can be transposed to express M_U at $x = l_0$ as

$$M_U(x = l_0) = M_N + (t+t_b)T_U/2.$$

Evaluating M_N from eqn (5.2) at $x = l_0$, setting $T_U = \bar{T}$ in the expression for M_U just given leads to

$$M_U(x = l_0^+) = \bar{T}\alpha l_0 + \bar{T}w$$

which satisfies the requirement that M_U in the overlap approaches the same value at $x = l_0$

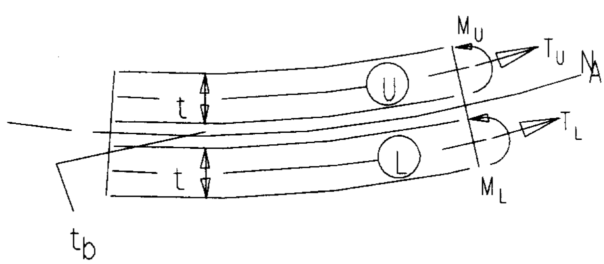

Fig. 5. Adherend moments and resultants.

as eqn (5.1) gives for the outer adherend, so that the present formulation maintains continuity of moment in the upper adherend, which was the main concern of Hart-Smith in Hart-Smith (1973). It will be seen later on in the discussion of peel stresses that the condition $M_L(x = l_0) = 0$ is also achieved, as a result of the boundary conditions on the peel stress expressions. In terms of deflections of the adherends, eqn (6) is equivalent to

$$M_N = D_U\left(\frac{d^2w_U}{dx^2}+\frac{d^2w_L}{dx^2}\right)-\frac{t+t_b}{2}(T_U-T_L); \quad D_U = E'\frac{t^3}{12} \tag{7.1}$$

in contrast with the classical bending–curvature relation used by GR:

$$M_N = \frac{E'h^3}{12}\frac{d^2w}{dx^2}. \tag{7.2}$$

In the above equations, M_N represents the moment about the neutral axis, w is lateral deflection and h is the height of the homogeneous beam model shown in Fig. 1(B)—i.e. approximately twice the adherend thickness, t, for a thin bond layer. With z as the thickness-wise coordinate having its origin at the mid-plane of the bond layer, the remaining quantities in eqns (6) and (7) are given by

$$M_N = -\int_{-h/2}^{h/2} z\sigma_x\,dz$$

$$M_U = \int_0^{h/2}(h/4-z)\sigma_x\,dz, \qquad M_L = -\int_{h/2}^{0}(z+h/4)\sigma_x\,dz$$

$$T_U = \int_0^{h/2}\sigma_x\,dz, \qquad T_L = \int_{-h/2}^{0}\sigma_x\,dz. \tag{8}$$

Equation (6), which is a statement of equilibrium in terms of the moments and resultants of the individual adherends, is equivalent to eqn (7.2), the classical beam equation used by GR, under certain conditions; however, these do not apply to the ends of the overlap where significant shear straining of the bond layer takes place. To see this it is necessary to compare eqn (7.1) with (7.2) as they apply to the case of a homogeneous beam. Assuming the validity of eqn (7.2) and equating h, the beam height, to $2t$, the z distribution of axial stress in the overlap region under combined bending and stretching is:

$$\sigma_x = \frac{\bar{T}}{2t}-\frac{M_N z}{I} \quad (\text{where } \bar{T} = T_L+T_U; \quad I = h^3/12 \equiv 2t^3/3). \tag{9}$$

Substituting (9) into (8) then leads to

$$M_U = M_L = E'\frac{t^3}{12}w'' \equiv \frac{1}{8}M_N; \qquad \frac{t}{2}T_L = \frac{t}{4}\bar{T}+\frac{3}{8}M_N \tag{10.1, 10.2}$$

$$\frac{t}{2}T_U = \frac{t}{4}\bar{T}-\frac{3}{8}M_N. \tag{10.3}$$

Since $t \approx h/2$, eqns (10) lead to

$$M_U + M_L + \frac{t}{2}(T_L - T_U) = \tfrac{2}{3}E't^3\frac{d^2w}{dx^2} \equiv \tfrac{1}{12}E'h^3\frac{d^2w}{dx^2} \tag{11}$$

which implies that eqns (10) have to hold in order for eqn (7.2) to be consistent with the equilibrium relation given by eqn (6). Note, however, that eqns (10) also lead to

$$M_U + M_L = \tfrac{1}{4}M_N; \qquad T_U - T_L = -\frac{3}{2t}M_N$$

implying that

$$T_U - T_L + \frac{6}{t}(M_U + M_L) = 0. \tag{12}$$

As a result, the following equation [see eqn (39) of GR], which gives the gradient of shear strain in the bond layer:

$$\frac{d\gamma}{dx} = \frac{1}{E'tt_b}\left[(T_U - T_L) + \frac{6}{t}(M_U + M_L)\right], \tag{13}$$

implies that the bond layer shear strain has to be a constant or zero for eqn (7.2) to hold. This is in obvious disagreement with the behavior of the joint near the ends of the overlap where the most significant shear strains can be expected. Equation (7.1), on the other hand, is completely consistent with (6) and therefore preserves the desired equilibrium statement in the formulation.

It is also noted that, as discussed in Hart-Smith (1973), eqns (10) which are required by the homogeneous beam equation (7.2), are in conflict with the conditions of zero traction and moment on the lower adherend at the left end of the overlap, as well as on the upper adherend at the right end. However, bending deflections in the overlap region are not the whole story with regard to satisfaction of end conditions on the adherends; thickness deflections of the bond layer due to the peel stresses, which were not taken into account in Hart-Smith (1973), add other considerations to the situation which will be discussed in the section below, where the analysis of Hart-Smith (1973) is treated in more detail.

The ensuing development will clarify the implications of the discrepancy between eqn (7.1) which allows for bond shear straining and thereby satisfies equilibrium in the form of eqn (6), and the classical beam equation (7.2) used by GR, which does not if bond shear strains are present.

DIFFERENTIAL EQUATIONS

Adherend constitutive relations

For the adherend moments and resultants we have

$$M_U = D_U w_{U,xx}; \quad M_L = D_L w_{L,xx}; \quad T_U = B_U u_{U,x}; \quad T_L = B_L \mu_{L,x}$$
$$D_U = D_L = \tfrac{1}{12}E't^3; \quad B_U = B_L = E't. \tag{14}$$

Deformations

Equating eqns (5.1) and (10.1) gives, for the left outer adherend, $0 \leqslant x \leqslant l_0$:

$$D_U \frac{d^2 w_U}{dx^2} = \bar{T}(\alpha x + w_U) \tag{15}$$

while for the overlap, making use of the notation of eqns (3) and equating eqn (5.2) with (7.1) gives

$l_0 \leqslant x \leqslant l + l_0$:

$$2D_U \frac{d^2 w}{dx^2} - \frac{t+t_b}{2} T_\Delta = \bar{T}w + \bar{T}\left(\alpha x - \frac{t+t_b}{2}\right). \tag{16}$$

For the right outer adherend ($x > l_0 + l$), displacements are determined by applying the antisymmetry conditions to the displacements of the left outer adherend.

Bond stresses and strains

Assuming the strains and stresses in the bond layer to be uniform through its thickness, the following expressions for strains are obtained [GR eqn (37)]:

$$\gamma_b = \frac{u_U - u_L}{t_b} + \frac{1}{2}\frac{t}{t_b}(w_{U,x} + w_{L,x}); \quad \varepsilon_b = \frac{w_U - w_L}{t_b} \tag{17.1}$$

with the shear and peel stress in the bond given by

$$\tau_b = G_b \gamma_b; \quad \sigma_b = E_b \varepsilon_b. \tag{17.2}$$

Note that eqn (13), which gives the gradient of shear strains, is obtained from the first of eqns (17.1) by differentiation and obvious substitutions involving eqns (14). Using eqns (17.2) to express the bond stresses in terms of the strains, eqn (13) can be stated as

$$\frac{d\tau_b}{dx} = \frac{G_b}{E'} \frac{1}{tt_b}\left[(T_U - T_L) + \frac{6}{t}(M_U + M_L)\right]. \tag{18}$$

Differential equation for adherend resultants

By equilibrium, the adherend resultants are related by the following expressions:

$$\frac{dT_U}{dx} = \tau_b; \qquad T_U + T_L = \bar{T}. \tag{19.1, 19.2}$$

Differentiating eqn (19.1), and making use of (4), (18) and (19.2) then gives

$$\frac{1}{2}\frac{d^2 T_\Delta}{dx^2} = \frac{G_b}{t_b}\left(\frac{1}{B_U} T_\Delta + t\frac{d^2 w}{dx^2}\right). \tag{20}$$

Peel stresses

In the GR analysis, the peel stresses were defined by a fourth-order differential equation which is reminiscent of the equation for a beam on an elastic foundation, of the form

$$\frac{d\sigma_b^4}{dx^4} + 4\frac{\gamma^4}{t^4}\sigma_b = 0 \quad \text{where} \quad \gamma = \left(\frac{E_b}{2D_U t_b}\right)^{1/4} t. \tag{21.1, 21.2}$$

Effects of the adherend deflections exist (Oplinger, 1991) which require modification of this equation for complete consistency with a beam response model for the adherends. However, practical limitations imposed by the structural capabilities of typical joint materials make the numerical effects of these modifications inconsequential, and the GR equation for the peel stresses will be retained here.

Combined equations

Displacement in outer adherend ($x \leqslant l_0$)

$$\frac{d^2 w_U}{dx^2} - \frac{U^2}{t^2} w_U = \frac{U^2}{t^2} \alpha x. \tag{22.1}$$

Displacement in overlapping segment of joint ($l_0 \leqslant x \leqslant l_0 + l$)

$$\frac{d^2 w}{dx^2} - \frac{1}{2}\frac{U^2}{t^2} w = \frac{1}{2}\frac{U^2}{t^2}\left(\alpha x - \frac{t+t_b}{2}\right) + \frac{t+t_b}{4}\frac{1}{D_U} T_\Delta. \tag{22.2}$$

Resultant difference ($x \leqslant l_0 \leqslant l_0 + l$)

$$\frac{d^2 T_\Delta}{dx^2} - 2\frac{\beta^2}{t^2} T_\Delta = 2G_b \frac{t}{t_b}\frac{d^2 w}{dx^2}. \tag{22.3}$$

The parameters U and β here are given by

$$U = t\sqrt{\bar{T}/D_U} \equiv \sqrt{12\bar{\varepsilon}_x}; \quad \beta = \sqrt{\rho_G/\rho_t} \quad \text{where} \quad \rho_G = G_b/E'; \quad \rho_t = t_b/t. \tag{23}$$

The ratio of U to β, denoted by R:

$$R \equiv \frac{U}{\beta} = \sqrt{12\frac{\bar{\varepsilon}_x \rho_t}{\rho_G}} \tag{24}$$

has an important influence on the results which follow.

SOLUTIONS

Solutions for w_U, w *and* T_Δ

When continuity at $x = l_0$ is allowed for, eqns (22) provide a coupled set of differential equations. Solutions can be expressed in the following form:

outer adherend displacement ($x \leqslant l_0$)

$$w_U = k\frac{t}{2}\frac{\sinh\left(U\frac{x}{t}\right)}{\sinh U\lambda_0} - \alpha x : \lambda_0 = \frac{l_0}{t}; \tag{25.1}$$

displacement in overlap region ($l_0 \leqslant x l_0 + l$)

$$w = \frac{t}{2}k_1\frac{\sinh[\mu_1(x-L)/t]}{\sinh(\mu_1\lambda/2)} + \frac{t}{2}k_2\frac{\sinh[\mu_2(x-L)/t]}{\sinh(\mu_2\lambda/2)} + \frac{t+t_b}{2} - \alpha x; \tag{25.2}$$

resultant difference ($l_0 \leqslant x \leqslant l_0 + l$)

$$T_\Delta = \left\{K_1 k_1\frac{\sinh[\mu_1(x-L)/t]}{\sinh(\mu_1\lambda/2)} + K_2 k_2\frac{\sinh[\mu_2(x-L)/t]}{\sinh(\mu_2\lambda/2)}\right\}\bar{T} \tag{25.3}$$

where

$$\lambda_0 = l_0/t; \quad \lambda = l/t \tag{25.4}$$

and where k, k_j, K_j and μ_j ($j = 1, 2$) are dimensionless parameters to be determined. In particular, μ_j, K_j and k_j are obtained from the solution of the following homogeneous system of differential equations:

$$D_{\mathrm{U}}\left(w_{\mathrm{h}}'' - \frac{U^2}{2t^2}w_{\mathrm{h}}\right) - \tfrac{1}{4}(1+\rho_{\mathrm{t}})T_{\Delta\mathrm{h}} = 0 \tag{26.1}$$

$$T_{\Delta\mathrm{h}}'' - 2\frac{\beta^2}{t^2}T_{\Delta\mathrm{h}} - 2\beta^2 E' w_{\mathrm{h}}'' = 0 \tag{26.2}$$

derived from eqns (22.2) and (22.3), together with the associated 2×2 system of linear equations given by

$$(2\mu_j^2 - U^2)E'\frac{t}{2}k_j - 6(1+\rho_{\mathrm{t}})K_j k_j \bar{T} = 0 \tag{27.1}$$

$$-2\beta^2\mu_j^2 E'\frac{t}{2}k_j + (\mu_j^2 - 2\beta^2)K_j k_j \bar{T} = 0 \tag{27.2}$$

corresponding to the solution of eqns (26) expressed as

$$w_{\mathrm{h}_j}(x) = k_j\frac{t}{2}\mathrm{e}^{\mu_j(x-L)/t}; \quad T_{\Delta\mathrm{h}_j} = K_j k_j \bar{T}\mathrm{e}^{\mu_j(x-L)/t}.$$

At this point the following notation is introduced

$$\mu_{G1} = \frac{U}{\sqrt{8}}; \quad \mu_{G2} = \sqrt{8}\,\beta \tag{28}$$

$$v_1 = \frac{\mu_1^2}{\beta^2}; \quad v_2 = \frac{\mu_2^2}{\beta^2}; \quad R_1 = \frac{\mu_1}{\mu_{G1}}; \quad R_2 = \frac{\mu_2}{\mu_{G2}}.$$

The parameters v_j ($j = 1,2$) are the roots of the following quadratic equation

$$v^2 - \left[8(1+\tfrac{3}{4}\rho_{\mathrm{t}}) + \frac{R^2}{2}\right]v + R^2 = 0 \tag{29}$$

which is the equivalent of setting the determinant of eqns (27) to zero. The roots of (29) are of the form

$$v_1, v_2 = a \mp b \quad \text{where} \quad a = \left[4(1+\tfrac{3}{4}\rho_{\mathrm{t}}) + \frac{R^2}{4}\right]; \quad b = \sqrt{a^2 - R^2}. \tag{30.1, 30.2, 30.3}$$

Once v_1 and v_2 are determined, the μ_js as well as the parameters R_j can be obtained from the definitions given in eqns (28).

With the values of μ_j determined, the corresponding K_js are obtained from either of eqns (27); in particular, eqn (27.2) gives

$$K_j = \frac{\beta^2 \mu_j^2}{\mu_j^2 - 2\beta^2} \frac{E't}{\bar{T}}$$

and, since the definition of U given in the first of eqns (23) implies that

$$E't = 12\frac{\bar{T}}{U^2},$$

then K_j can be expressed as

$$K_j = \frac{12}{U^2} \frac{\beta^2 \mu_j^2}{\mu_j^2 - 2\beta^2}. \tag{31}$$

It should be noted that, since the product of the roots of a quadratic is equal to its constant term, eqn (29) implies that $v_1 v_2 = R^2$, which can be shown to require that

$$R_2 \equiv 1/R_1. \tag{32}$$

Using this and other relationships, K_1 and K_2 are given by

$$K_1 = \frac{3}{4} \frac{1}{\frac{R^2}{16} - R_2^2}; \quad K_2 = \frac{48}{R^2} \frac{R_2^2}{4R_2^2 - 1}. \tag{33}$$

Once these parameters are determined, the final expressions for w_U in the outer adherend together with w and T_Δ in the overlap region are obtained by allowing for continuity of w, dw/dx and T_U at $x = l_0$, which requires the following set of equations:

$$K_1 k_1 + K_2 k_2 = -1 \tag{34.1}$$

$$k_1 + k_2 + k = 1 + \rho_t \tag{34.2}$$

$$R_1 R k_1 + 8R_2 \frac{T_{h21}}{T_{h22}} k_2 - \sqrt{8}\, R \frac{T_{h21}}{T_{h1}} k = 0 \tag{34.3}$$

where

$$T_{h2j} = \tanh(\mu_j \lambda/2); \quad T_{h1} = \tanh(U\lambda_0). \tag{34.4}$$

Note that eqns (34) imply that the w and dw/dx are equal to w_U and $dw_U dx$ at l_0. In accordance with the discussion following eqn (54) below regarding the effects of thickness deflections of the bond layer, this is not strictly true, since a difference between w and w_U amounting to $t_b\sigma_b/2E_b$ is present. To be completely correct, ρ_t in eqn (34.2) needs to be replaced by $(1 + t_b\sigma_b/2E_b)\rho_t$, while the quantity 0 on the right side of (34.3) needs to be replaced by $t_b\,(d\sigma_b/dx)/2E_b$. There will be similar correction terms in the expression for k given in eqn (36.1) below. These terms could be accommodated by obtaining σ_b from the peel stress solution; however, it will be found that their effect on the displacement is only about 1% of t_b for bonds loaded to less than their failure strains in bond thickness deformation; a similar level of effect will be found for the derivative of σ_b to be added to the right side of eqn (34.1) as well as in the numerator of (36.1). It is true that the bond thickness deformation effects are needed conceptually to circumvent the Hart-Smith concern about discontinuities in the axial adherend stresses; however, their effect on predicted bending displacements as well as the stresses in the bond layer appear too small to bother about.

Proceeding with the solution of eqns (34), denoting

$$C_1 = K_1/K_2; \quad C_2 = 1/K_2 \tag{35}$$

then the solution for k, k_1 and k_2 can be expressed as

$$k = \left(R_1 R(1+\rho_t+C_2) - 8R_2\frac{T_{h21}}{T_{h22}}[C_1(1+\rho_t)+C_2]\right) \times \left(\frac{T_{h1}}{T_{h1}\left(R_1 R - 8R_2\frac{T_{h21}}{T_{h22}}C_1\right)+\sqrt{8}R(1-C_1)T_{h21}}\right) \tag{36.1}$$

$$k_1 = \frac{1+\rho_t+C_2-k}{1-C_1}; \qquad k_2 = -(C_1 k_1 + C_2). \tag{36.2, 36.3}$$

Because of antisymmetry, the deflection beyond the overlap ($x > l_0+1$) in the lower adherend is given by $w_L(l-x) = -w_U(x)$.

For most practical situations, the value of R obtained from (24) will be of the order of 1 or less while the quantity "a" given in (30.2) cannot be less than four, so that in general we have $R^2 \ll a^2$. Accordingly, a binomial expansion of (30.3) gives the approximation

$$b \approx a - R^2/2a \tag{37}$$

which is within 1% of the exact expression given by eqn (30.3) for all positive values of R. Accordingly, eqn (37) is an acceptable substitute for (30.3).
Equation (30.1) together with (28) then leads to

$$v_2 = 2a - \frac{R^2}{2a}; \quad R_2 = \sqrt{\frac{a}{4} - \frac{R^2}{16a}}; \quad R_1 = 1/R_2 \tag{38.1}$$

$$\mu_1 = R\beta \Big/ \sqrt{2a - \frac{R^2}{2a}}; \quad \mu_2 \approx \sqrt{2a - \frac{R^2}{2a}}\,\beta. \tag{38.2}$$

According to the definitions of R_1 and R_2 given in (28) together with those of $\mu_{Gj} (j = 1, 2)$, for large adherend thickness for which $\rho_t \ll 1$, this leads to

$$\mu_1 \approx R\frac{\beta}{\sqrt{8}} \equiv \mu_{G1}; \quad \mu_2 \approx \sqrt{8}\,\beta \equiv \mu_{G2} \tag{39}$$

which are the roots of the original GR analysis.

In addition, as indicated in eqn (24), R tends toward zero for large t, so that all the terms in eqn (36.1) containing R as a factor will disappear, while R_1 and R_2 approach unity. We then have:

$$t \gg t_b, (R, \rho_t \to 0)$$

$$k \to \frac{(1+\rho_t)T_{h1}}{T_{h1} + \sqrt{8}(1+3\rho_t/2)T_{h21}} \tag{40}$$

which, as discussed later, is equivalent to the expression for k obtained by GR after modification for (1) finite outer adherend length and (2) the parameter ρ_t allowing for non-zero bond thickness. (The significance of the latter was pointed out to the writer in a private communication from Tsai and Morton.) In other words, eqn (40) is consistent with original GR analysis when applied to relatively thick adherends.

In addition to the expression for k, we also wish to examine the expressions for K_1 and K_2. Substituting eqn (30.2) into (38.2) and the result into (33) gives, for the case of $t_b t \ll 1$,

$t \gg t_b(R, \rho_t \to 0)$

$$K_1 \approx -\frac{3}{4+3\rho_t}; \quad K_2 \approx \frac{16}{R^2}\frac{1}{1+\rho_t}. \tag{41}$$

From (41) it is apparent that we can set

$$K_1 \approx -3/4; \quad K_2 \approx 16/R_2 \quad (t \gg t_b). \tag{42}$$

Substituting (41) into (35) and the result into (36.2, 36.3) leads to

$t \gg t_b(R, \rho_t \to 0)$

$$k_1 \approx 1-k; \quad k_2 \approx \frac{R^2}{16}[\tfrac{3}{4}(1-k)-1] \approx 0 \tag{43}$$

and applying (41) and (43) to (25.3) then leads to

$t \gg t_b(R, \rho_t \to 0)$

$$K_1 k_1 \bar{T} \approx -\tfrac{3}{4}(1-k)\bar{\sigma}_x t; \quad K_2 k_2 \bar{T} \approx -\frac{1+3k}{4}\bar{\sigma}_x t \tag{44}$$

which may be substituted into eqn (25.3) to obtain the appropriate approximation for T_Δ in the case of thick adherends. This is used subsequently to obtain the GR shear stress expression.

BOND LAYER STRESSES

Shear stresses

The bond layer shear stress distribution is obtained from substituting eqn (25.3) into (4) to obtain T_U and differentiating the resulting expression to allow for (19.1), which leads to:

$$\tau_b = \left\{\frac{\mu_1}{2t}K_1 k_1 \frac{\cosh[\mu_1(x-L)/t]}{\sinh(\mu_1\lambda/2)} + \frac{\mu_2}{2t}K_2 k_2 \frac{\cosh[\mu_2(x-L)/t]}{\sinh(\mu_2\lambda/2)}\right\}\bar{T}. \tag{45}$$

For the case of $t \gg t_b$, making use of eqns (44) for expressing $K_j k_j$ leads to

$t \gg t_b(R, \rho_t \to 0)$

$$\tau_b \approx \bar{\sigma}_x \left\{\frac{\sqrt{8}\beta}{8}(1+3k)\frac{\cosh[\sqrt{8}\beta(x-L)/t]}{\sinh(\sqrt{8}\beta\lambda/2)} + \frac{3}{8\sqrt{8}}U(1-k)\frac{\cosh[U(x-L)/\sqrt{8}t]}{\sinh(u\lambda/2\sqrt{8})}\right\}$$

from which the maximum value of shear stress in the bond layer is approximately

$t \gg t_b(R, \rho_t \to 0)$

$$\frac{\tau_b|_{\max}}{\bar{\sigma}_x} \approx \frac{\sqrt{8}\beta}{8}(1+3k)\frac{1}{\tanh\left(\sqrt{8}\beta\frac{\lambda}{2}\right)} + \frac{3}{8\sqrt{8}}U(1-k)\frac{1}{\tanh\left(U\frac{\lambda}{\sqrt{8}}\right)}. \tag{46}$$

In the special case in which the overlap length is relatively small so that $U\lambda/(2\times 8^{1/2}) \ll 1$, it will be found that

$$\tanh\left(U\frac{\lambda}{2\sqrt{8}}\right) \approx U\frac{\lambda}{2\sqrt{8}}$$

in which case eqn (45) becomes

$$\frac{\tau_b|_{\max}}{\bar{\sigma}_x} \approx \frac{\sqrt{8}\beta}{8}(1+3k)\frac{1}{\tanh\left(\sqrt{8}\beta\frac{\lambda}{2}\right)} + \frac{3}{4}\frac{(1-k)}{\lambda} \tag{47}$$

which is the GR expression for the maximum shear stress.

Peel stresses

The solution to eqns (21) for the peel stresses is straightforward, and is given by

$$\sigma_b(x) = \sigma_c Cc + \sigma_s Ss \tag{48}$$

where σ_c and σ_s are constants determined from the end conditions on M_U, M_L, V_U, and V_L which are described in the last four rows of Table 1, while $Cc(x)$ and $Ss(x)$ are given by

$$Cc(x) = \cosh\left(\gamma\frac{x-L}{t}\right)\cos\left(\gamma\frac{x-L}{t}\right); \quad Ss(x) = \sinh\left(\gamma\frac{x-L}{t}\right)\sin\left(\gamma\frac{x-L}{t}\right). \tag{49}$$

Expressions for the derivatives of Cc and Ss which are needed subsequently, are given by

$$\frac{dCc}{dx} = \frac{\gamma}{t}[Sc(x) - Cs(x)]; \quad \frac{dSs}{dx} = \frac{\gamma}{t}[Sc(x) + Cs(x)] \tag{50.1}$$

where

$$Sc(x) = \sinh\left(\gamma\frac{x}{t}\right)\cos\left(\gamma\frac{x}{t}\right); \quad Cs(x) = \cosh\left(\gamma\frac{x}{t}\right)\sin\left(\gamma\frac{x}{t}\right). \tag{50.2}$$

The following notation represents the values of these functions at the end of the overlap where $x = l_0 + l$:

$$P_1 \equiv \frac{t}{\gamma}\frac{dSs}{dx}\bigg|_{x-l_0+l}; \quad P_2 = \frac{t}{\gamma}\frac{dCc}{dx}\bigg|_{x=l_0+l}; \quad P_3 = Ss|_{x=l_0+l}; \quad P_4 = Cc|_{x=l_0+l} \tag{51}$$

$$\Delta = P_1 P_4 - P_2 P_3 \equiv \tfrac{1}{2}[\sinh(2\gamma\lambda) + \sin(2\gamma\lambda)].$$

The expression for the peel stresses is then given by

$$\sigma_b(x) = \frac{1}{\Delta}\frac{\bar{T}\gamma}{t}\left\{\left(P_2\frac{k}{2}\gamma+P_4\frac{k}{2}U\right)Cc(x)+\left(P_1\frac{k}{2}\gamma+P_3\frac{k}{2}U\right)Ss(x)\right\} \tag{52}$$

which is the expression given by GR. The maximum value of the peel stress occurs at the ends of the overlap where $x = l_0+1$, leading to

$$\sigma_b\big|_{\max} = \bar{\sigma}_x\gamma\left\{\frac{k\gamma}{2}\frac{(P_2P_4+P_1P_3)}{\Delta}+\frac{kU}{2}\frac{(P_4^2+P_3^2)}{\Delta}\right\}. \tag{53}$$

For most practical joints, γ is large enough so that $\gamma\lambda \gg 1$, in which case
$\gamma l/t \gg 1$

$$\sigma_b\big|_{\max} \approx \bar{\sigma}_x\frac{k\gamma}{2}(\gamma+U). \tag{54}$$

A word should be mentioned here regarding the effect of bond layer thickness deflections on the adherend axial tractions at the ends of the overlap. The end conditions on the peel stress equation, which are taken from the last four rows of Table 1, are specifically designed to add the effect of thickness deformations of the bond to the average of the adherend displacements given by w. Note that the thickness displacement of the bond is given by $t\sigma_b/E_b$ which leads to expressions for the displacements of the individual adherends as follows:

$$w_U = w+\frac{1}{2}\frac{t_b}{E_b}\sigma_b; \quad w_L = w-\frac{1}{2}\frac{t_b}{E_b}\sigma_b.$$

The terms involving σ_b here do not show up in the quantity M_U+M_L which appears in eqn (6) for M_N, since they cancel out. Accordingly, eqn (22.2) for bending deflection in the overlap region does not show an effect of bond thickness deformations, other than a small contribution to the moment distribution [see the remarks following eqns (5)] which is ignored. On the other hand, while the thickness deformation $t_b\sigma_b/E_b$ may be small enough to ignore, the quantity $D_Ut_b(d^2\sigma_b/dx^2)$ may be substantial and, in fact, is determined by the end conditions given in Table 1 to satisfy the requirement $M_L = M_U-M_0$ at $x = l_0$, insuring that $M_L = 0$ as well as $V_L = 0$ there; the conditions $M_U = 0 = V_U$ are similarly insured at the right end of the joint by the requirements stated in Table 1. Note that the evaluation of the GR analysis given by Hart-Smith did not include the contributions of bond thickness deformations to the end conditions in the overlap, and needs to be re-examined.

CORRECTIONS TO THE GOLAND–REISSNER ANALYSIS FOR BOND THICKNESS EFFECTS

It is desirable at this point to provide a correction to the original GR analysis which takes into account effects of non-zero bond layer thickness, since comparison with the analysis introduced in the present paper would be misleading without taking these effects into account. The GR analysis used a version of eqn (5.2) in which $t+t_b$ was replaced by t, thus ignoring the effect of t_b on the moment distribution in the overlap region. Furthermore, setting h to $2t$ in eqn (7.2), which was done in GR, implies that the flexural rigidity D_N of the homogeneous beam used to represent the overlap region does not allow for the presence of the bond layer. For consistency with the analysis introduced in the present paper, the following expression for D_N is needed:

$$D_N = \tfrac{2}{3}E'\left[\left(t+\frac{t_b}{2}\right)^3-\left(\frac{t_b}{2}\right)^3\right]+E_b\frac{t_b^3}{12}$$

which is the flexural rigidity of a layered beam having an inner layer of modulus E_b and thickness t_b surrounded by two identical layers of modulus E' and thickness t. The last expression is equivalent to

$$D_N = 8C_\rho D_U \quad \text{where} \quad C_\rho = 1+\tfrac{3}{2}\rho_t+\tfrac{3}{4}\rho_t^2+\frac{\rho_t^3}{8}\frac{E_b}{E'}. \tag{55}$$

In the GR analysis, C_ρ was replaced by 1. The introduction of C_ρ in eqn (55) and use of eqn (5.2) for the moment distribution gives the GR equivalent of eqn (22.2) as

$$w''-\frac{1}{8C_\rho}\frac{U^2}{t^2}w = \frac{1}{8C_\rho}\frac{U^2}{t^2}\left(\alpha x-\frac{1+\rho_t}{2}t\right). \tag{56}$$

Providing continuity of w and dw/dx at $x = l_0$ then leads to the modified GR expression for k, denoted k_{GRc} (i.e. the "corrected" GR expression for k), given by

$$k_{GRc} = \frac{\tanh U\lambda_0}{\tanh U\lambda_0+\sqrt{8C_\rho}\tanh(U\lambda/2\sqrt{8C_\rho})}(1+\rho_t)$$

or, using the version of the latter which assumes that the outer adherend is long enough to set $\tanh(U\lambda_0) \approx 1$ as GR did,

$$k_{GRc} = \frac{1}{1+\sqrt{8C_\rho}\tanh(U\lambda/2\sqrt{8\lambda})}(1+\rho_t). \tag{57}$$

Setting ρ_t to zero and C_ρ to 1 in eqn (57) recovers the original GR expression for k.

COMMENTS ON THE HART-SMITH ANALYSIS

To date, the only serious attempt to correct the deficiencies of the GR bending deflection analysis, other than the present one, appears to have been that of Hart-Smith (1973) which was developed on a NASA contract in the early 70s. Hart-Smith's subsequent publications have frequently quoted the results obtained in that source, and a comparison with the present analysis is in order.

There are two issues to be considered here. The first is the concern with an apparent violation of end conditions on the individual adherends by the GR beam model. Hart-Smith's point of view on this is clarified in pp. 15–18 of Hart-Smith (1973), particularly by Fig. 4 of that reference which suggests that the GR homogeneous beam model implies the presence of non-zero tractions at the left end of the lower adherend as well as at the right end of the upper adherend, where they should be zero. However, as the discussion of the present paper following eqn (54) points out, the correct end conditions on the adherends are, in fact, provided for as boundary conditions stated in Table 1 for the beam-on-elastic-foundation equation (22.1), which is really an equation for the bond thickness deformation. On the other hand [again as noted in the discussion following eqn (54)], whatever beam model is used for predicting the bending deflections in the overlap, the effects of bond thickness deformations cancel out there since only the sum of the displacements enters. Thus the axial stress distribution implied by the composite beam model for bending deflections of the overlap are not relevant to the end conditions on the individual adherends, so that the Hart-Smith concern with traction conditions on the individual adherends implied by the GR beam model does not appear to be valid.

The second consideration here is the bending deflection analysis of Hart-Smith (1973). To examine this, we note that the following expressions for beam shear forces on the individual adherends, eqn (7) of that reference (using the sign conventions and notation of the present paper) are used:

$$\frac{t+t_b}{2}\tau_b - \frac{dM_U}{dx} = V_U\,; \quad \frac{t+t_b}{2}\tau_b - \frac{dM_L}{dx} = V_L. \tag{58}$$

Making use of eqns (19) here, which requires that $dT_U/dx = -dT_L/dx = \tau_b$, and adding the two members of eqns (58) leads to

$$\frac{t+t_b}{2}\frac{d(T_L-T_U)}{dx} + \frac{d(M_U+M_L)}{dx} = -(V_U+V_L).$$

Making use of eqn (6), this is equivalent to

$$\frac{dM_N}{dx} = -(V_U+V_L) \tag{59}$$

or, since by equilibrium (Goland and Reissner, 1944) $V_U+V_L = \bar{V}$, this formulation leads to

$$dM_N/dx = -\bar{V}$$

from which

$$M_N(x) = -\bar{V}x + \text{const.} \tag{60}$$

Since [see eqns (2)] $\bar{V}$ is equivalent to $-\bar{T}\alpha$, eqn (60) is equivalent to eqn (5.2) without the presence of the term involving w.

This is not the equation used in Hart-Smith (1973) for the bending deflection analysis, however. That analysis used a differentiated form of eqn (59) involving the derivatives of V_U and V_L, which are related (Goland and Reissner, 1944) to the bond layer peel stresses by

$$\frac{dV_U}{dx} = \sigma_b\,; \quad \frac{dV_L}{dx} = -\sigma_b. \tag{61}$$

Note again that there is no influence of bending deflection on the moments given by these expressions, even though the complete moment distribution expression given in eqn (5.2) requires it. The Hart-Smith bending analysis was then equivalent to differentiating eqn (59) and allowing for eqns (61) to get a fourth-order equation of the form

$$\frac{d^4w}{dx^4} = \tfrac{1}{2}(t_b+t)\frac{1}{D_U}\tau_{b,x} \tag{62}$$

with the solution given, using present notation, in the form

$$w = \frac{t+t_b}{D_U}\frac{A_2t^3}{8(\sqrt{2}\beta)^3}\sinh[\sqrt{2}\beta(x-L)/t] + A_3(x-L)^3 + C_3(x-L) \tag{63}$$

where k, together with A_1, A_3 and C_3 are unknowns to be determined from continuity of displacement, slope and curvature as well as the derivative of the shear stress at the ends of the overlap. The following expression for k is obtained by Hart-Smith when these conditions are satisfied:

Table 2. Comparison of GR[1] and present notation

Present	GR
l_0	l
$l/2$	c
$L\ (\equiv l_0+l/2)$	$l+c$
D_u	D_1
$D_u/(8)^{1/2}$	D_2
U/t	u_1
$U/(8)^{1/2}t$	u_2
t_b	η
G_b, E_b	G_c, E_c
E'	$E/(1-\nu^2)$
$\bar{\sigma}_x$	p
$\beta=(G_b t/E' t_b)^{1/2}$	$\beta=(8G_b t/E' t_b)^{1/2}$
$(\lambda U/4T_{h1})k$	k'

$$k=\frac{\text{NUM}}{\text{DEN}}$$

where

$$\text{NUM}=1+\frac{1}{64}R^2\left[1+\frac{1}{3}(\sqrt{2}\beta\lambda)^2-\frac{\sqrt{2}\beta\lambda}{\tanh\sqrt{2}\beta\lambda}\right]$$

$$\text{DEN}=1+U\frac{\lambda}{2}+\frac{1}{6}\left(U\frac{\lambda}{2}\right)^2+\frac{3}{64}R^2\left[1+\frac{1}{3}(\sqrt{2}\beta\lambda)^2-\frac{\sqrt{2}\beta\lambda}{\tanh\sqrt{2}\beta\lambda}\right]. \tag{64}$$

The final expression used by Hart-Smith for calculations of k are the approximation obtained when the terms in eqns (64) involving R^2 are eliminated as being too small to be considered. The following results:

$$k_{\text{HS}}=\frac{1}{1+U\frac{\lambda}{2}+\frac{1}{6}\left(U\frac{\lambda}{2}\right)^2}, \tag{65}$$

i.e. the inverse of a polynomial in the expression $U\,\lambda/2$.

The absence of the effect of bending deflections in eqns (59) and (61) completely changes the character of the solution. As a result, the influence of adherend deflections predicted by this approach gives much longer range effects than those of the present analysis.

Considering k as a function of $U\lambda/2\equiv(12\bar{\varepsilon}_x)^{1/2}l/2t$, i.e. dimensionless overlaps length times half the square root of the loading strain, the GR analysis has the well-known lower limit $k\approx 0.262$ for large $U\lambda/2$. In addition, as seen in the next section, both the corrected GR expression of eqn (57) and the modification for bond shear strain effects given in eqns (36) will lead to a non-zero lower limit on k for large $U\lambda/2$, although in this case it varies from the GR limit of 0.262. In contrast, the Hart-Smith expression reaches a lower limit of zero for increasing $U\lambda/2$. Note that because of the significant departure of the Hart-Smith k prediction from those of the GR and present analyses, it results in unrealistically low peel stresses for large overlaps as well as in shear stresses which are considerably lower than the other analyses will give.

NUMERICAL RESULTS

Before proceeding, it is worthwhile to provide a comparison of the notation of the present paper with that used by Goland and Reissner, for ease in interpreting the implications of the present analysis. The comparison is given in Table 2.

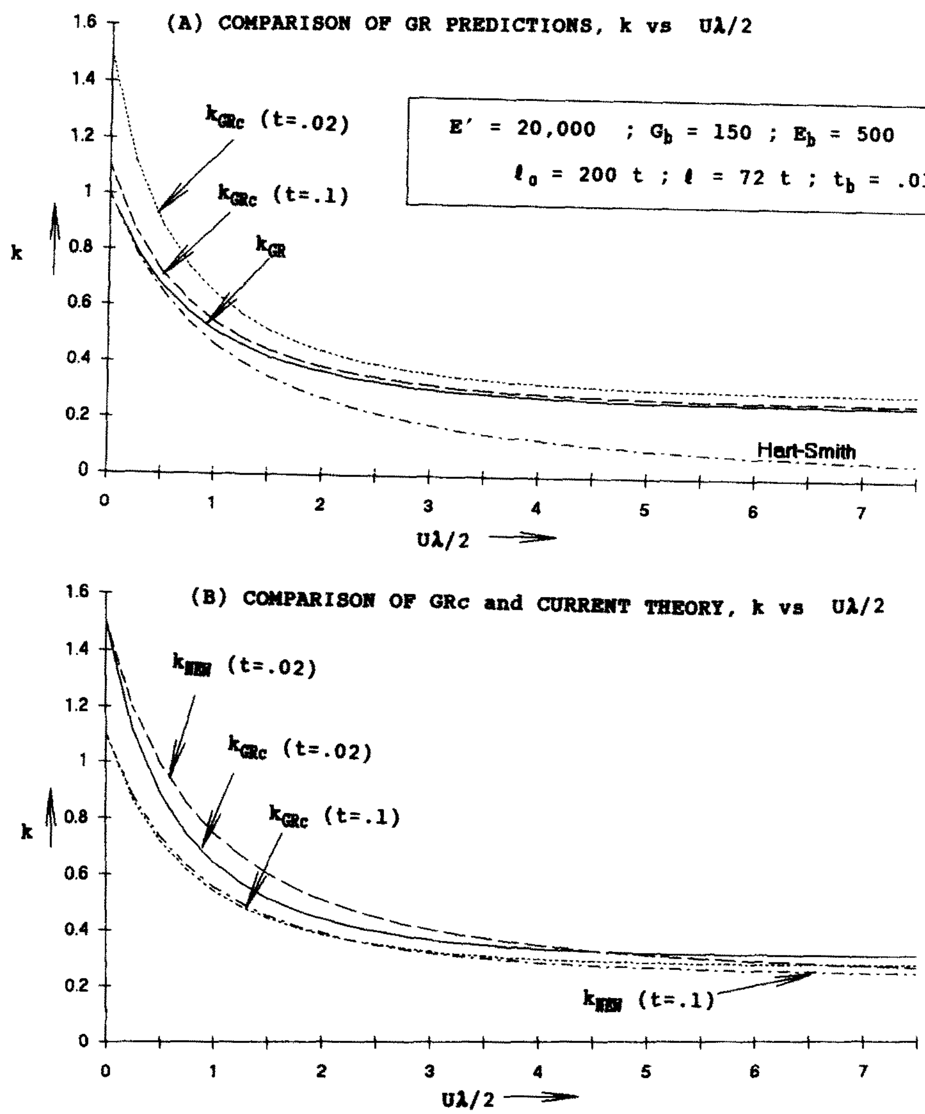

Fig. 6. Comparison of predictions—k vs $U\lambda/2$.

Curves of k_{GRc} vs $Ul/2$ are compared with the GR prediction ("k_{GR}"), as well as the Hart-Smith prediction, for various ρ_t in Fig. 6(A), while the comparison of k predicted by the currrent theory, denoted "k_{NEW}", with the k_{GRc}, is given in Fig. 6(B). Figure 7 clarifies the relationship between $\bar{\sigma}_x$ and $U\lambda/2$ for various axial adherend moduli.

Figure 8 gives a comparison of shear and peel stress predictions for the current theory and the GR theory corrected for bond layer thickness.

Table 3 clarifies the differences in the predictions of various quantities for $\bar{\sigma}_x = 50$ and $l = 72t$. Note the terminology "bss" referring to the model developed here to account for the effect of bond layer shear strain on the bending deflection, corresponding to eqns (36) for k and (46) for the maximum shear stress. In particular, the difference between the "GRc" and "bss" predictions is about 19% for $t = 0.02$ vs 14% for $t = 0.1$, for both k and $\sigma_b|_{\max}$; for $\tau_b|_{\max}$, the corresponding differences amount to 11% and 4%, respectively.

CONCLUSIONS

In the context of the use of beam theory for modelling adherend bending response, the approach employed in this paper appears to provide a more consistent model than that of

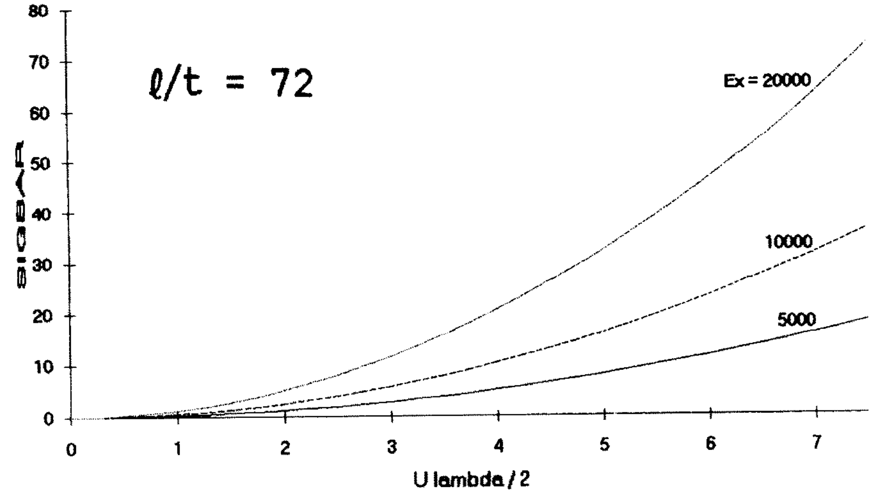

Fig. 7. $\bar{\sigma}_x$ vs $U\lambda/2$ for adherends of various axial moduli.

GR by adding the effects of bond shear strains. The present analysis is admittedly incomplete in ignoring the effects of bond thickness deformation as they influence the continuity conditions at the ends of the overlap as well as the moment distribution along the overlap; however, these effects appear to be inconsequential in terms of their effect on either the dimensionless displacement parameter k or the influence of k on the bond stress predictions.

It is re-emphasized that the original Goland–Reissner model, in analysing the deflections of the joint, used a classical homogeneous beams model for calculating the bending deflections, which was not consistent with the bi-layer model used by them, to predict bond shear and peel stresses. Due to the long range nature of the effect of bond shear strains on the bending stiffness of the joint when the adherends are thin, the largest differences between the present approach and the GR approach occur in the case of thin adherends. On the other hand, the numerical results which have been obtained demonstrate that the original GR approach produces numerical results which do not differ greatly from those of the present analysis for large adherend thicknesses; in such cases the effects which are ignored in the GR approach are so concentrated near the ends of the overlap that their consequences are not significant. Thus, for thicker adherends, the GR approach can be considered to have been satisfactory from the standpoint of sound engineering. The insight that Goland and Reissner brought to bear on the effects of adherend bending deflections together with the role of peel stresses on the strength of adhesive joints still stand as a major advance in the understanding of factors important to successful adhesive joint design.

In regard to the analysis given in Hart-Smith (1973), the concern that the GR model led to incorrect end conditions on the individual adherends, ignored the effects of thickness deformations of the bond layer which were explicitly provided by GR, and does not appear to be valid. Moreover, neglect of the effects of bending deflections on the overlap moment distribution in Hart-Smith (1973) led to an invalid expression for the dimensionless moment, $k\bar{T}t/2$, which radically departs from those of both GR and the present analysis for long overlaps.

As noted in the Introduction, the intent of the present analysis was to retain the analytically simple beam model used by GR which incorporated classical beams for the adherends and a thickness-wise uniform distribution of stresses in the bond layer, as a means of re-evaluating the issues raised by Hart-Smith. Accordingly, a number of details of joint behavior have not been addressed here and should be brought into consideration. Transverse shear deformations in the adherends in addition to ductile response of the bond layer need to be accounted for; these have been addressed by the writer and will be the subject of future publications. In addition, a number of issues regarding the details around the end of the joint, especially the effect of the adhesive fillet, need to be examined further. Efforts such as those of Adams (1989) and Adams and Wake (1984) as well as Tsai and Morton (1993) have provided considerable insight into these effects.

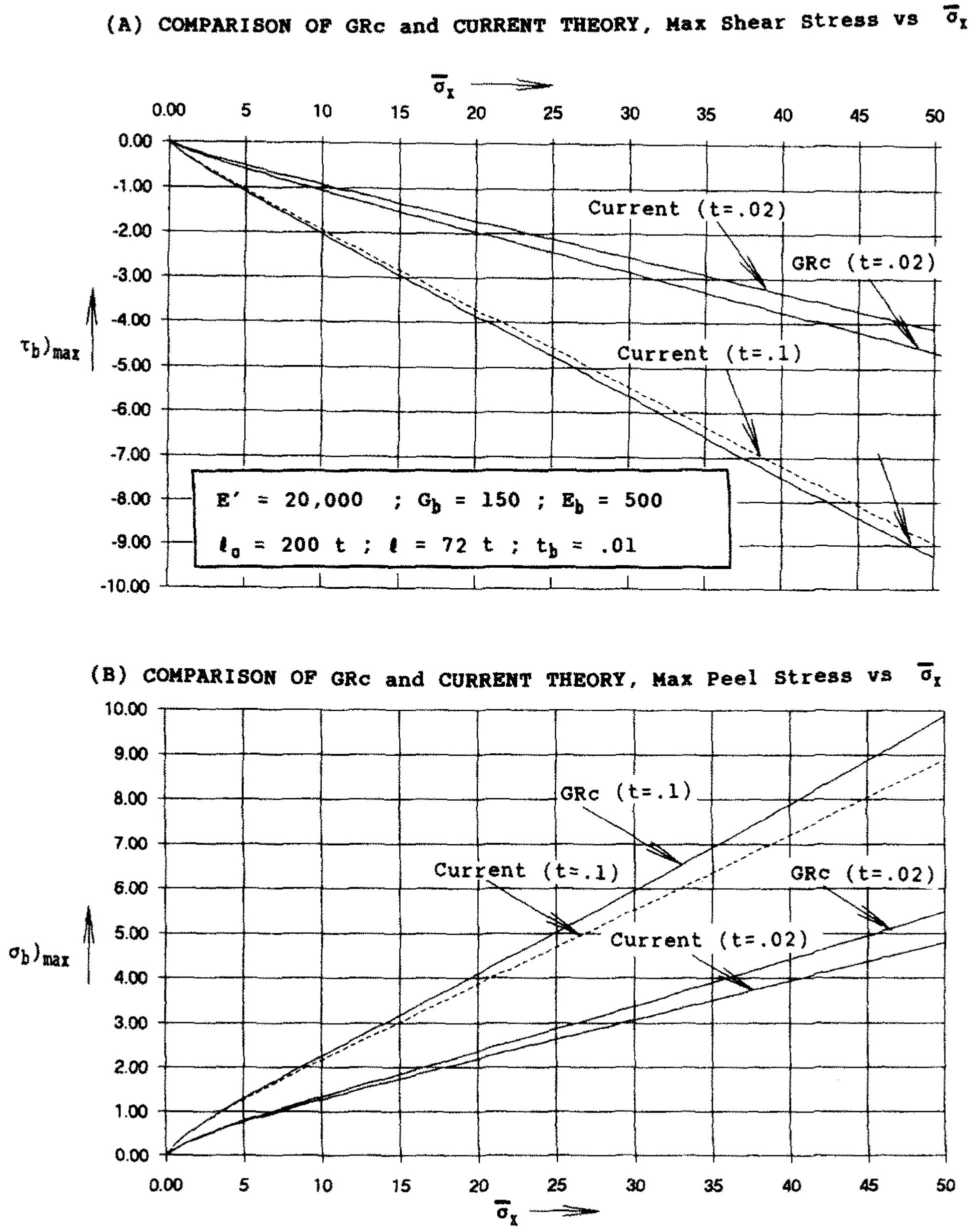

Fig. 8. Bond layer stresses vs $\bar{\sigma}_x$.

Table 3. Comparison of results for $\bar{\sigma}_x = 50$, $l = 72t$ ($E' = 20{,}000$, $G_b = 150$, $t_b = 0.01$, $\lambda_0 = 20$)

Prediction	GR ($t = 0.02$)	GRc ($t = 0.02$)	"bss" model† ($t = 0.02$)	GR ($t = 0.1$)	GRc ($t = 0.1$)	"bss" model† ($t = 0.1$)
k value	0.263	0.315	0.264	0.263	0.275	0.241
$\tau_b\|_{max}$	4.346	4.62	4.15	9.278	9.31	8.92
$\sigma_b\|_{max}$	4.427	5.56	4.65	9.278	9.90	8.68

†"bss" model—bond shear strain model, eqns (36), (46) and (53).

REFERENCES

Adams, R. D. (1989). Strength predictions for lap joints, especially with composite adherends. A review. *J. Adhesion* **30,** 219–242.

Adams, R. D. and Wake, W. C. (1984). *Structural Adhesive Joints in Engineering.* Elsevier Applied Science, London.

Benson, N.K. (1969). Influence of stress distribution on strength of bonded joints. In *Adhesion, Fundamentals and Practice*, pp. 191–205. Gordon and Breach, New York.

Carpenter, W. (1989). Goland and Reissner were correct. *J. Strain Anal.* **24,** 185–187.

Carpenter, W. (1991). A comparison of numerous lap joint theories for adhesively bonded joints. *J. Adhesion* **35,** 53–73.

Goland, M. and Reissner, E. (1944). Stresses in cemented joints. *ASME J. Appl. Mech.* **11,** A17–A27.

Hart-Smith, L. J. (1973). Adhesive bonded single lap joints. NASA Contractor Report 112236.

Hart-Smith, L. J. (1981). In *Developments in Adhesives*, Vol. 2 (Edited by A. J. Kinloch). Elsevier Applied Science, London.

Kuenzi, E. and Stevens, G. (1963). Determination of mechanical properties of adhesives for use in the design of bonded joints. Forest Products Laboratory Note FPL-011.

Kutscha, D. and Hofer, K. (1968). Feasibility of joining advanced composite flight vehicle structures. Air Force Materials Laboratory Report AFML-TR-68-391, pp. 56–59.

Oplinger, D. W. (1991). A layered beam theory for single-lap joints. U.S. Army Materials Technology Laboratory Report MTL TR 91-23.

Snedon, I. (1962). The distribution of stress in adhesive joints. In *Adhesion*, Chapter 9 (Edited by D. D. Eeley). Oxford University Press, Oxford.

Tsai, M. Y. and Morton, J. (1993). *Proc. 18th Annual Air Force Mechanics of Composites Review*, U.S. Air Force Wright Aeronautical Laboratories, Dayton, OH.

Tsai, M. Y. and Morton, J. (1994b). An evaluation of analytical and numerical solutions to the single-lap joint. *Int. J. Solids Structures* **31,** 2537–2563.